Local quantum control of Heisenberg spin chains

Rahel Heule,[1] C. Bruder,[1] Daniel Burgarth,[2,3] and Vladimir M. Stojanović[1,*]

[1] *Department of Physics, University of Basel, Klingelbergstrasse 82, CH-4056 Basel, Switzerland*
[2] *Institute for Mathematical Sciences, Imperial College London, SW7 2PG, United Kingdom*
[3] *QOLS, The Blackett Laboratory, Imperial College London, Prince Consort Road, SW7 2BW, United Kingdom*

(Dated: September 7, 2010)

Motivated by some recent results of quantum control theory, we discuss the feasibility of local operator control in arrays of interacting qubits modeled as isotropic Heisenberg spin chains. Acting on one of the end spins, we aim at finding piecewise-constant control pulses that lead to optimal fidelities for a chosen set of quantum gates. We analyze the robustness of the obtained results for the gate fidelities to random errors in the control fields, finding that with faster switching between piecewise-constant controls the system is less susceptible to these errors. The observed behavior falls into a generic class of physical phenomena that are related to a competition between resonance- and relaxation-type behavior, exemplified by motional narrowing in NMR experiments. Finally, we discuss how the obtained optimal gate fidelities are altered when the corresponding rapidly-varying piecewise-constant control fields are smoothened through spectral filtering.

PACS numbers: 03.67.Hk, 03.67.Lx, 75.10.Pq

I. INTRODUCTION

The ability to manipulate the state and/or the dynamics of complex quantum systems is one of the main objectives of quantum information science [1]. In this context, quantum control [2] has been successfully utilized to address two general classes of issues. In *state-selective* control, the main question is how to steer a physical system from an initial reference state to a desired final state. In *operator (state-independent)* control, one seeks to implement a predetermined unitary transformation (target quantum gate) irrespective of the initial state of the system, which is often unknown. The rigorous mathematical foundations of the field, based on the notion of controllability and framed using Lie-algebraic concepts, have long been known [3]. Recent quantum-control studies have been focused around two sets of questions.

Firstly, even when a system is fully controllable in principle, it is of interest to know how to control it most efficiently, taking into account various practical constraints. Issues of this type are not likely to yield universal answers, except for well-understood general topological features of optimal-control landscapes [4]. Secondly, it is desirable to know whether the system can be partly or fully controlled by acting only on a small subsystem. This is the main idea behind the *local-control* (minimal actuation) approach. Such an approach is applicable only in interacting systems like coupled spin chains, where the interaction will effectively turn the local control applied to the small subsystem to a global one. Uses of such "always-on" interactions in quantum information processing include, e.g., systems which can serve as data buses [5] enabling state- [6–9] and entanglement transfer [10]. Several notable results have recently been reported [11–14]. For instance, controlling only one of the end spins of an XXZ-Heisenberg spin chain ensures full controllability of the chain [12]. In addition, universal quantum computation with the XY spin chain can be effected by controlling two spins at the end of the chain [13]. Finally, a magnetic field in the z-direction acting only on a single spin suffices for generating perfect entanglement between the ends of a Heisenberg chain [14].

Apart from being interesting from a conceptual point of view, the local-control approach also has some practical importance. In addition to its easier implementation, lowering the number of control actuators reduces the effects of decoherence. This is of crucial importance in many quantum-computer architectures, such as superconducting qubits [15, 16].

In this paper, motivated in part by the rigorous results of Ref. 12, we consider an implementation of local operator control in arrays of interacting qubits modeled as spin chains with isotropic Heisenberg interaction. Acting only on one of the end spins, we determine piecewise-constant control fields resulting in the highest possible fidelities for a chosen set of quantum gates. By treating the amplitudes of these control fields as optimization variables, we find the optimal fidelities for chains with up to four spins [17]. While our work focuses on Heisenberg-coupled spin chains, its results are relevant for any physical implementation of interacting qubit arrays.

While some elements of the quantum control of spin chains have already been studied [18] – even in the open-system scenario [19] – we discuss in detail some aspects that have so far not received due attention. In particular, we carry out a sensitivity analysis, i.e., consider the robustness of the obtained results for the gate fidelities with respect to random errors in the control fields. Our analysis shows that with faster switching between piecewise-constant controls, the system is less suscepti-

*Electronic address: vladimir.stojanovic@unibas.ch

ble to these errors. Importantly, we explain this behavior by making a link to a class of phenomena exemplified by motional narrowing in NMR experiments [20]. To bridge the gap between theoretical considerations and future experimental implementations of the system under study, we discuss how the optimal fidelities are affected when the control pulses are smoothened by eliminating high-frequency components in their Fourier spectra (spectral filtering). We establish some qualitative criteria regarding the performance of such an approach.

The paper is organized as follows. To set the stage, in Sec. II we introduce the system and our control objectives. In Sec. III we present detailed results for the optimal gate fidelities and the corresponding control fields in chains with three and four spins. We also discuss minimal action times for the control fields needed to realize certain quantum gates. Section IV is set aside for the sensitivity analysis, while Sec. V deals with the effects of spectral filtering of the optimal piecewise-constant control fields on the resulting gate fidelities. We conclude with a brief summary of the paper and some general remarks in Sec. VI. Some numerical details are described in Appendix A.

II. SYSTEM AND METHOD

A. Hamiltonian and control objectives

We consider an isotropic Heisenberg spin-1/2 chain of length N_s, with control fields acting on the first spin only. It is governed by the total Hamiltonian

$$H(t) = H_0 + H_c(t)\,, \tag{1}$$

where H_0 is the Heisenberg Hamiltonian

$$H_0 = J\sum_{i=1}^{N_s-1}\left(S_{ix}S_{i+1,x} + S_{iy}S_{i+1,y} + S_{iz}S_{i+1,z}\right)\,, \tag{2}$$

while

$$H_c(t) = h_x(t)S_{1x} + h_y(t)S_{1y} \tag{3}$$

is the Zeeman-like control Hamiltonian. The time dependence of the control fields $h_x(t)$ and $h_y(t)$ will be specified shortly. For convenience, throughout this paper we set $\hbar = 1$. As a consequence, all frequencies and control-field amplitudes can be expressed in units of the coupling strength J, and all times in units of $1/J$.

Regarding the choice of Hamiltonian in Eq. (2) two remarks are in order. Firstly, while the algebraic result of Ref. 12 is even applicable to the more general (anisotropic) XXZ-Heisenberg Hamiltonian, for simplicity we here discuss the isotropic case only. Secondly, whether the spin chain is ferromagnetic ($J < 0$) or antiferromagnetic ($J > 0$) is unessential for our present purposes, because we are concerned with operator control. For concreteness we assume that $J > 0$.

In Ref. 12, using the graph infection criterion, it was shown that controlling the x and y components of the field acting on the first spin guarantees the complete controllability of a Heisenberg chain. Moreover, there are unitary transformations that require even smaller degree of control, i.e., a control field only in one direction. For instance, to achieve a spin-flip operation X on the last spin of the chain, where X is the Pauli matrix, one needs only a control field in the x direction. The corresponding dynamical Lie algebra $\mathcal{L}_x$, generated by $\{-iH_0, -iS_{1x}\}$, is a subalgebra of $su(d)$. The action of the N_s-qubit gate X_{N_s}, which flips the last spin in the Heisenberg chain, is defined by

$$X_{N_s} := \mathbb{1}\otimes\mathbb{1}\otimes\ldots\otimes\mathbb{1}\otimes X\,. \tag{4}$$

To prove the reachability of X_{N_s}, i.e., that $X_{N_s} \in e^{\mathcal{L}_x}$ [where $e^{\mathcal{L}_x}$ is the connected Lie subgroup of $SU(d)$ with Lie algebra $\mathcal{L}_x$], we have to show that there exists an element A of the dynamical Lie algebra $\mathcal{L}_x$ such that $X_{N_s} = e^A$. By calculating the (repeated) commutators of the operators which generate the algebra, we find that X_{N_s} is an element of $\mathcal{L}_x$. Since X_{N_s} is both unitary and Hermitian (hence $X_{N_s}^2 = \mathbb{1}$), the operator $A = -i\frac{\pi}{2}X_{N_s}$, an element of $\mathcal{L}_x$, has the property that $e^A = -iX_{N_s}$. This concludes the proof that the x field is sufficient to reach X_{N_s}. More generally, any unitary U, which is also Hermitian and for which $-iU$ belongs to the dynamical Lie algebra $\mathcal{L}$, is an element of the reachable set $e^{\mathcal{L}}$.

In the following, our control objective is the realization of concrete quantum gates. We discuss gates that require control fields in the x and y directions, as well as those that entail only an x control field. Apart from spin-flip (NOT) gates, we implement entangling two-qubit gates such as

$$\mathrm{CNOT}_{N_s} := \mathbb{1}\otimes\mathbb{1}\otimes\ldots\otimes\mathbb{1}\otimes\mathrm{CNOT}\,, \tag{5}$$

which performs the controlled-NOT (CNOT) operation on the last two qubits in the chain. Another example is square root of SWAP ($\sqrt{\mathrm{SWAP}}$). In operator control, the figure of merit in the realization of these gates is the gate fidelity

$$F(t) = \frac{1}{d}\left|\mathrm{tr}\left[U^\dagger(t)U_{\mathrm{target}}\right]\right|\,, \tag{6}$$

where $U(t)$ is the time-evolution operator of the system at time t and U_{target} stands for the desired quantum gate.

B. Time-evolution for piecewise-constant control fields

For many classes of systems, the implementation of complicated time-dependent potentials is rather difficult. In what follows, we resort to simple piecewise-constant controls. Importantly, we retain the full Hilbert space of the system, unlike some previous studies that make use of

the single-excitation subspace. [21] This puts constraints on the system size.

Assume that we want to achieve an arbitrary target unitary at a time $t = t_f$. At $t = 0$ we apply an x control pulse to the first spin of the chain with amplitude $h_{x,1}$ which is constant throughout the pulse duration T. That is, the system evolves under the action of the Hamiltonian $H_{x,1} \equiv H_0 + h_{x,1}S_{1x}$. Then we apply a y control pulse with amplitude $h_{y,1}$ during the second time interval of length T, whereby the system is governed by the Hamiltonian $H_{y,1} \equiv H_0 + h_{y,1}S_{1y}$. This sequence of alternate x and y control pulses is repeated until N_t pulses have been completed at the time $t_f \equiv N_t T$. The full time-evolution operator can be expressed as

$$U(t_f) = U_{y,N_t/2} \cdot U_{x,N_t/2} \cdot ... \cdot U_{y,1} \cdot U_{x,1} \,, \qquad (7)$$

where $U_{x,i} \equiv e^{-iH_{x,i}T}$ and $U_{y,i} \equiv e^{-iH_{y,i}T}$ are the respective time-evolution operators corresponding to $H_{x,i}$ and $H_{y,i}$. We evaluate $U_{x,i}$ and $U_{y,i}$ using their spectral forms. If the desired gate is achievable by control of the x field only, it is sufficient to apply in each time interval an x field of variable amplitude.

III. THREE- AND FOUR-SPIN CHAINS

For the numerical maximization of the fidelity [Eq. (6)] with respect to the N_t field amplitudes, we use a quasi-Newton method developed by Broyden, Fletcher, Goldfarb, and Shanno (BFGS-algorithm) [22]. We first choose an initial guess for the control-field amplitudes. The algorithm then generates iteratively new sequences of field amplitudes such that at each iteration point the fidelity is increased, and terminates as soon as the desired accuracy is reached. This procedure ensures the convergence to a local maximum, but of course does not guarantee the convergence to a globally-optimal sequence of control field amplitudes.

We perform maximizations with varying number N_t and durations T of pulses, and hence different total evolution times $t_f = N_t T$. It is important to stress that, instead of fixing the pulse durations and maximizing over the field amplitudes, we could as well keep the amplitudes constant and treat the pulse durations as free control parameters [11, 23]. Yet, we choose to maximize over the field amplitudes as this approach allows us to fix easily the total evolution time and estimate its minimal value needed to implement the desired gate. Although controllability implies the existence of a control that can enable realization of a desired quantum gate, it does not provide any information about the minimal time over which this realization is possible.

We now give explicit examples of control sequences that implement all of our chosen gates in chains of three and four spins, among them entangling gates which are essential for universal quantum computation. Two optimal sequences of control pulses implementing the spin-flip gate X_{N_s} for a three-spin chain ($N_s = 3$) with x and y pulses are shown in Fig. 1 [the optimal field in Fig. 1(b) corresponds to the minimal time needed]. For given total time longer than the minimal time, we can generate piecewise-constant control fields with fidelities arbitrarily close to unity by increasing the switching rate. For instance, in the case of implementing the gate X_3 by control of the x and y fields, for a total time of $t_f = 30$ and $N_t = 10, 20, 30, 40, 50, 60, 70$, we respectively obtain $F = 0.536, 0.764, 0.904, 0.964, 0.992, 0.999, 1 - 10^{-8}$.

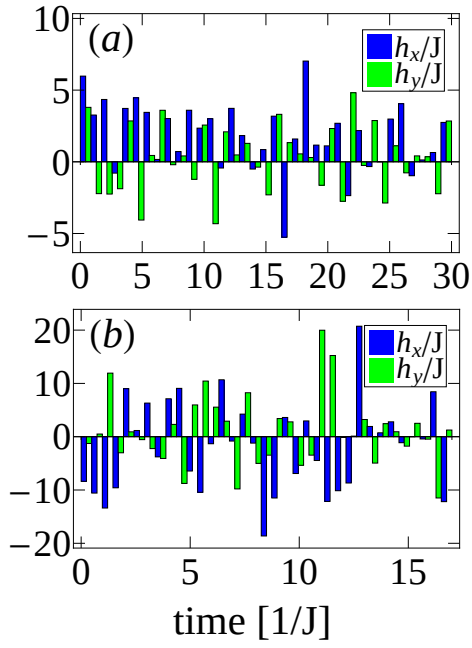

FIG. 1: (Color online) Examples of optimal control fields for the X_3 gate, corresponding to: (a) $N_t = 70$ and $T = 0.429$, with the resulting optimal fidelity of $1 - 10^{-8}$, and (b) $N_t = 70$ and $T = 0.243$ (minimal total time $t_f = 17$), with the resulting optimal fidelity of $1 - 10^{-6}$.

We give here an estimate of the minimal time for the realization of the gate X_{N_s} (operating on three- and four-spin chains) by controlling the x and y field. The implementation of this unitary is possible with a maximal gate error of 10^{-2} for $N_s = 3$ and $N_s = 4$ within the respective times $t_f = 17$ and $t_f = 70$, which are lower bounds on the evolution time needed. Unlike in Ref. 13, the size of the dynamical Lie algrebra scales exponentially with the number of qubits. We therefore expect that the minimal time grows rapidly with the chain length, and this is a limiting factor for extending this control procedure.

For each fixed chain length, the minimal times for realizing different gates (spin-flip, CNOT, $\sqrt{\text{SWAP}}$) are similar. This result seems somewhat related to the main conclusion of Ref. 24, where the CNOT gate is implemented for two qubits coupled through a variety of interactions (XY, Heisenberg, Ising) and the total gate time does not depend significantly on the choice of interaction as long as it is not of pure Ising type.

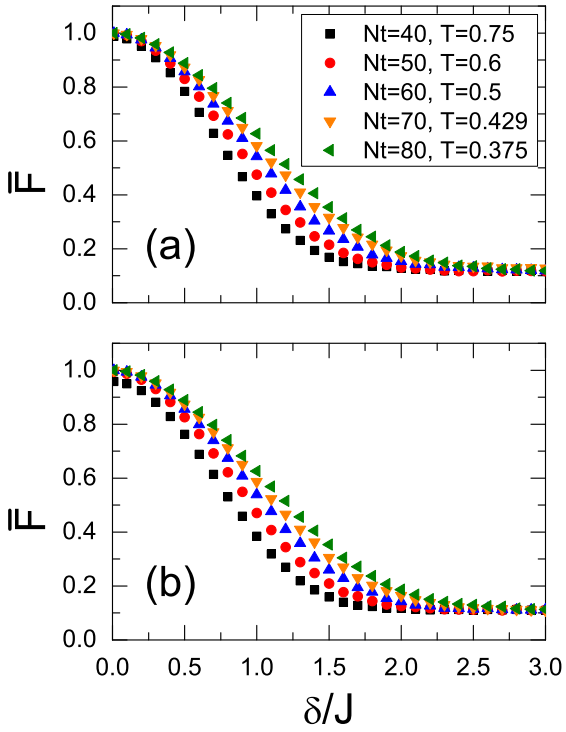

FIG. 2: (Color online) Average fidelity versus half-width (δ) for random noise affected optimal fields corresponding to (a) X_3 gate, and (b) CNOT$_3$ gate, both implemented by alternate x and y controls with a total evolution time $t_f = 30$.

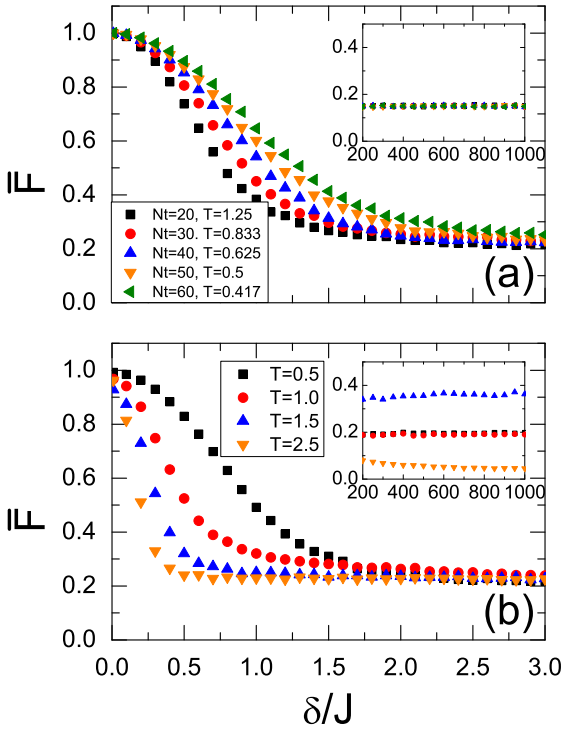

FIG. 3: (Color online) Average fidelity versus half-width (δ) for random noise affected optimal fields corresponding to the implementation of the X_3 gate by control of the x field only: (a) fixed total evolution time ($t_f = 25$) and (b) fixed number of pulses ($N_t = 70$). The insets show the same curves for large values of the parameter δ.

Recalling that gates like X_{N_s} require only an x control field, it is interesting to compare the minimal times for their implementation depending on the degree of control. We find that with control of the x field only, the respective gates can be achieved in approximately the same time as with control of both the x and y fields.

IV. SENSITIVITY ANALYSIS

A. Preliminary considerations

In the following, we analyze the sensitivity of the fidelity to random errors in the control fields. To this end, we add random numbers from a uniform distribution of half-width δ to the optimal control-field amplitudes. For given δ, we generate a few hundred sequences of random numbers. In this way we obtain a large sample of $N \sim 1000$ control fields affected by random noise, for which we recalculate the fidelity. We note that the standard deviation σ_F increases with δ: for $\delta = 0.01$ it is found to be of the order of 10^{-5}, while for $\delta = 1.0$ we obtain $\sigma_F \sim 0.1$.

In the following, we discuss the behavior of the average fidelity $\bar{F} = \sum_{i=1}^{N} F_i/N$, where the F_i are fidelities calculated for specific realizations of the random field. Figures 2 and 3 illustrate how the strength of the randomness in the optimal field amplitudes affects the average fidelity. While Fig. 2 shows the results for the gates X_3 and CNOT$_3$ both realized by a sequence of alternate x and y pulses, Fig. 3 refers to the implementation of X_3 by control of the x field only. We see that $\bar{F}$ is less susceptible to random noise for shorter pulse durations T. A physical understanding of this phenomenon is provided in Sec. IV C.

Starting from optimal fields, the shape of the fidelity decay with increasing δ is dependent on the number of control pulses N_t and their length T, but not on the pulse amplitudes. The saturation regime of the average fidelity sets in for $\delta \gtrsim J$, thus indicating full randomization. Importantly, the saturation of the fidelity is an intrinsic property of our system. If the system is completely controllable, the saturation value is universal, i.e., independent of the concrete shape of the control field, provided the evolution time t_f and the number of pulses N_t allow the generation of any unitary (illustrated in Fig. 2 for $t_f = 30$). In contrast, if the dynamical Lie algebra of the system is a proper subalgebra of $su(d)$, for different evolution times t_f the average fidelity may saturate at different values, and the saturation may require much stronger random fields in comparison to the completely controllable system (for illustration, see Fig. 3).

B. Fidelity saturation

To understand the value of the fidelity at saturation, we invoke the notion of the average gate fidelity [25]. If ε is a trace-preserving quantum operation pertaining to a quantum system with d-dimensional Hilbert space and U a certain quantum gate, the average gate fidelity

$$\bar{F}(\varepsilon, U) = \frac{\sum_{j=1}^{d^2} \mathrm{tr}\left[U U_j^\dagger U^\dagger \varepsilon(U_j)\right] + d^2}{d^2(d+1)} , \qquad (8)$$

where $\{U_j\}$ is an orthonormal unitary-operator basis of the complex vector space $\mathbb{C}^{d\times d}$, quantifies how well ε approximates U. If ε implements the gate U perfectly, this mapping is given by $\varepsilon : \rho \to \varepsilon(\rho) = U\rho U^\dagger$, implying that $\bar{F}(\varepsilon, U) = 1$; otherwise, the implementation is noisy and, consequently, $\bar{F}(\varepsilon, U) < 1$. An equivalent form of Eq. (8) – which involves the traceless generators $\{T_j\}$ of $SU(d)$ [recall that $\mathrm{tr}(T_j T_k) = \delta_{jk}/2$, see e.g. Ref. 26] reads [27]:

$$\bar{F}(\varepsilon, U) = \frac{1}{d} + \frac{2}{d(d+1)} \sum_{j=1}^{d^2-1} \mathrm{tr}\left[U T_j U^\dagger \varepsilon(T_j)\right] . \qquad (9)$$

Equations (8) and (9) are both derived by integrating over the uniform Haar measure [25], hence requiring a uniform starting distribution of states and/or operators. Since the quantum control system governed by the Hamiltonian $H(t) = H_0 + h_x(t)S_{1x} + h_y(t)S_{1y}$ allows to generate any element of $SU(d)$, Eq. (9), which is derived explicitly in terms of the $SU(d)$ group generators, provides a suitable expression for calculating the average gate fidelity. Assuming that the condition of full randomization is fulfilled, the action of the quantum operation ε is given by

$$\varepsilon : \rho \to \varepsilon(\rho) = \frac{\mathbb{1}}{d} \qquad (10)$$

for every ρ, that is, an arbitrary (pure) state is mapped onto a maximally-mixed state. We recall that an arbitrary density matrix can be written as

$$\rho = \frac{\mathbb{1}}{d} + \sum_{j=1}^{d^2-1} a_j T_j \quad (a_j \in \mathbb{R}) . \qquad (11)$$

Since $\varepsilon(\rho) = \mathbb{1}/d$ for an arbitrary ρ, by assumption, it follows by linearity and trace-preserving that $\varepsilon(T_j) = 0$, for every $j = 1, \ldots, d^2 - 1$. Hence, the sum in Eq. (9) evaluates to 0, implying that the average gate fidelity for the mapping in Eq. (10) is given by

$$\bar{F}(\varepsilon, U) = \frac{1}{d} . \qquad (12)$$

Note that Eq. (12) is applicable only if the randomness in the control field amplitudes allows the uniform generation of any unitary contained in $SU(d)$. For example, in the three-spin ($d = 8$) case we expect the average gate fidelity to saturate at a value of 0.125. This seems to be numerically corroborated by Fig. 2 and indicates that the system undergoes full randomization. Also in a four-spin chain ($d = 16$), provided that full randomization occurs, the found saturation value fits well with $1/d = 0.0625$ (not illustrated here). It should be emphasized that this regime of full randomization is of no relevance for practical realizations of control, however, it provides an important consistency check of our numerical results.

We now address the observation that there exists no universal saturation value in the case of control by x pulses only, see Fig. 3. This type of control does not allow universal quantum computation, i.e., the reachable set of unitary operators is reduced to a Lie subgroup of $SU(d)$. Since Eq. (8) is only valid if the reachable set equals the full $SU(d)$, the reasoning leading to Eq. (12) does not apply to such a subgroup. The accessible part of the reachable set depends on the evolution time t_f. The control fields of Fig. 3(b) differ in t_f which may result in different accessible parts of the reachable sets and, consequently, different saturation values. The fact that in Fig. 3(a), where all fields have the same t_f, the average gate fidelity saturates to the same value corroborates this explanation.

C. Physical interpretation

As illustrated in Figs. 2 and 3, the average fidelity is less susceptible to random errors for shorter time intervals T. This is a special case of a more general physical situation, namely a competition between resonance- and relaxation-type behavior [28]. A typical example is the phenomenon of motional narrowing of the linewidth in NMR experiments [20].

This generic class of phenomena is discussed based on models for a randomly-interrupted deterministic motion [28]: a system is subjected to a random event (e.g., switching between magnetic fields B_0 and $-B_0$ in NMR) with the switching rate λ, while in between two random events it evolves deterministically. On the whole, the system is then evolving piecewise-deterministically and its qualitative behavior depends on the relative magnitude of the switching rate λ and the average (absolute) external field amplitude (B_0 in the example above). Note that with units chosen such that $\hbar = 1$ both quantities have the same physical dimensions.

In our system, for smaller time intervals T the fidelity in the presence of random errors is indeed closer to the intrinsic optimal values. Interestingly, $\lambda = T^{-1} \sim J$ in the optimal cases, while the average (absolute) control-field amplitudes (that are independent of δ because of the symmetry of the probability distribution) are of the same order of magnitude. This explains the dependence of $\bar{F}$ on δ: the fidelity varies significantly with δ and saturates at a value around 0.125 in the case of a completely con-

trollable three-spin chain (0.0625 in the four-spin chain). In contrast to that, for λ much bigger than the average control-amplitudes, the fidelities would remain close to 1 even for large δ.

V. SPECTRAL FILTERING

Our choice of piecewise-constant control fields is, at least partly, a matter of mathematical convenience. In realistic implementations of quantum control various constraints may come into play, the most important ones pertaining to the complexity of the frequency spectrum of permissible control fields. In control experiments that make use of an external magnetic field, for instance, such constraints are related to bandwidth and slew-rate limitations of the magnetic coils and drivers [29]. Therefore, it is necessary to subject the optimal control fields to spectral filtering in order to make contact with experimental realizations [30].

In what follows, we aim at finding control fields that are smoother than the optimal piecewise-constant ones, at the same time retaining high fidelities for our target quantum gates. To this end, we put constraints on the frequency spectra of the control fields $h_j(t)$ $(j = x, y)$ by means of frequency filter functions. After operating with a filter function $f(\omega)$ on the Fourier transforms $\mathcal{F}[h_j]$ of the optimal fields, we switch back to the time domain and calculate the filtered control fields $\widetilde{h}_j(t)$ via inverse Fourier transformation [31]:

$$\widetilde{h}_j(t) = \mathcal{F}^{-1}\big[f(\omega)\mathcal{F}[h_j](\omega)\big](t) \quad (j = x, y)\,. \tag{13}$$

The power spectrum of a typical optimal piecewise-constant control field is depicted in Fig. 4.

Based on the obtained smoothened control fields, we calculate the corresponding fidelities for different quantum gates, using a product-formula approximation (for details, see Appendix A).

We first consider an *ideal low-pass* filter which removes frequencies outside the interval $[-\omega_0, \omega_0]$: $f(\omega) = \theta(\omega + \omega_0) - \theta(\omega - \omega_0)$. Using the general prescription in Eq. (13), we obtain

$$\begin{aligned} \widetilde{h}_x(t) &= \frac{1}{\pi}\sum_{n=1}^{N_t/2} h_{x,n}\big[a_{2n-1}(t) - a_{2n-2}(t)\big]\,, \\ \widetilde{h}_y(t) &= \frac{1}{\pi}\sum_{n=1}^{N_t/2} h_{y,n}\big[a_{2n}(t) - a_{2n-1}(t)\big]\,, \end{aligned} \tag{14}$$

where $a_m(t) \equiv \mathrm{Si}\big[\omega_0(mT - t)\big]$ and $\mathrm{Si}(x) \equiv \int_0^x (\sin t/t)dt$. Two examples of such smoothened pulses for the X_3 and CNOT_3 gates, corresponding to a fidelity of 0.9, are shown in Figs. 5 and 6.

We also consider *Gaussian filters* with center frequencies $\pm\omega_c$: $f(\omega) = \exp[-\gamma(\omega - \omega_c)^2] + \exp[-\gamma(\omega + \omega_c)^2]$, where $\gamma > 0$ determines the Gaussian full-width-at-half-maximum FWHM $= 2\sqrt{\ln 2/\gamma}$. As the power spectra

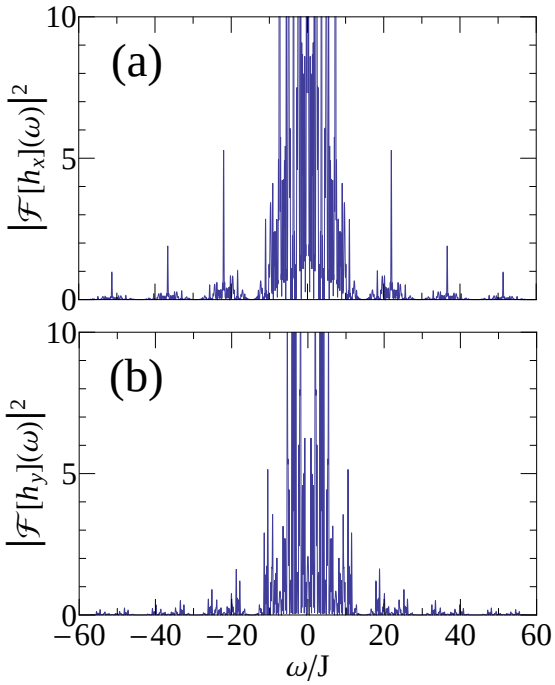

FIG. 4: (Color online) The power spectra corresponding to the optimal x [(a)] and y [(b)] control fields shown in Fig. 1(a).

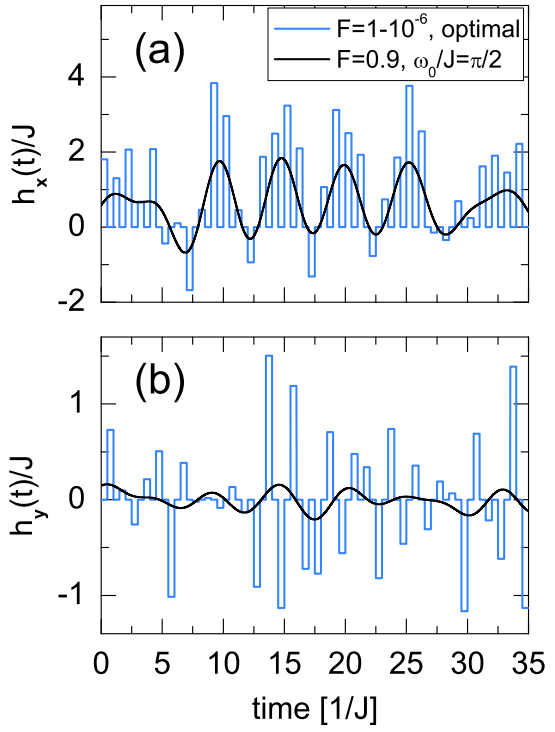

FIG. 5: (Color online) Optimal piecewise-constant control field which realizes the X_3 gate by alternate x [(a)] and y [(b)] pulses, compared to the low-pass filtered counterpart (cut-off frequency $\omega_0/J = \pi/2$) with a fidelity of 0.9. The optimal field corresponds to $N_t = 70$ and $T = 0.5$.

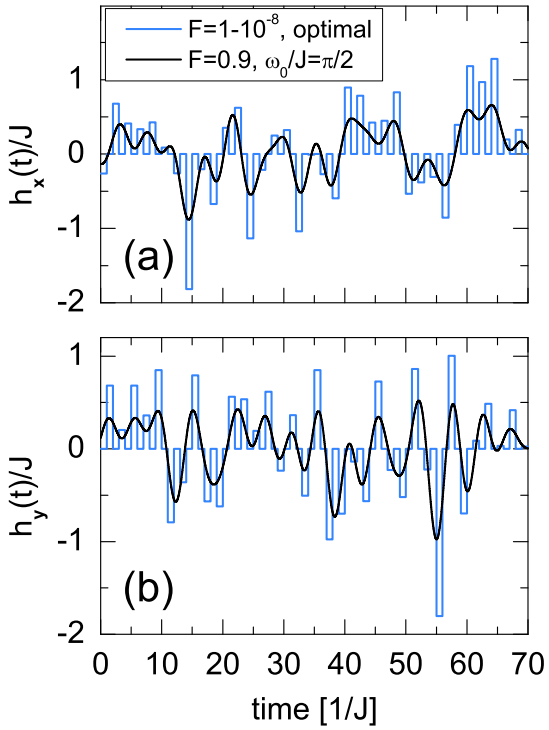

FIG. 6: (Color online) Optimal piecewise-constant control field which realizes the CNOT_3 gate by alternate x [(a)] and y [(b)] pulses, compared to the low-pass filtered counterpart (cut-off frequency $\omega_0/J = \pi/2$) with a fidelity of 0.9. The optimal field corresponds to $N_t = 70$ and $T = 1.0$.

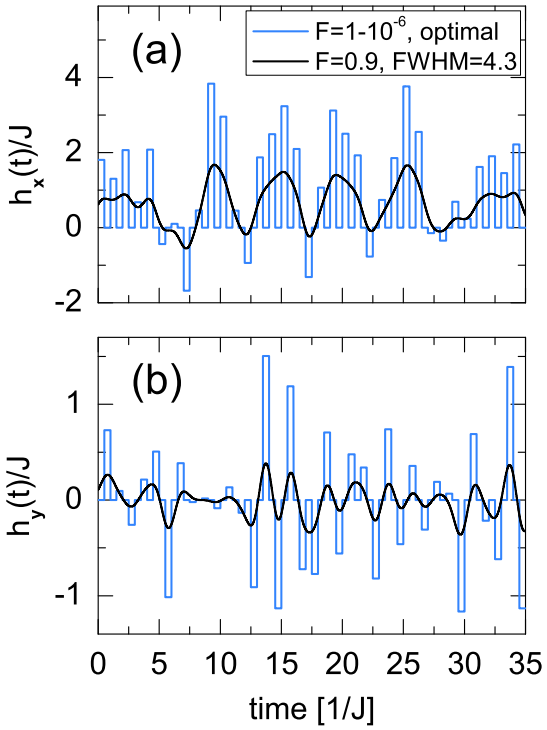

FIG. 7: (Color online) Optimal piecewise-constant control field which realizes the X_3 gate by alternate x [(a)] and y [(b)] pulses, compared to the Gaussian filtered counterpart (FWHM = 4.3) with a fidelity of 0.9. The optimal control field corresponds to $N_t = 70$ and $T = 0.5$ as in the case of low-pass filtering shown in Fig. 5.

of the optimal control fields (Fig. 4) show, the dominant frequencies are located around $\omega = 0$. Hence we choose $\omega_c = 0$ and vary the Gaussian width. We determine the smoothened control fields by making use of the identity [32]

$$\int_0^\infty e^{-p^2x^2} \frac{\sin(ax)}{x}\, dx = \frac{\pi}{2}\,\mathrm{erf}\left(\frac{a}{2p}\right), \qquad (15)$$

where erf is the error function. We obtain

$$\begin{aligned} \widetilde{h}_x(t) &= \frac{1}{2}\sum_{n=1}^{N_t/2} h_{x,n}\left[b_{2n-1}(t) - b_{2n-2}(t)\right], \\ \widetilde{h}_y(t) &= \frac{1}{2}\sum_{n=1}^{N_t/2} h_{y,n}\left[b_{2n}(t) - b_{2n-1}(t)\right], \end{aligned} \qquad (16)$$

where $b_m(t) \equiv \mathrm{erf}\left[(mT - t)/(2\sqrt{\gamma})\right]$. The results obtained through Gaussian filtering resemble the ideal low-pass ones. In Fig. 7 we show the optimal sequence of controls realizing the X_3 gate which is now smoothened by applying a Gaussian filter, however retaining a fidelity of 0.9 (compare the corresponding low-pass filtered pulse in Fig. 5).

The behavior of the fidelity versus the cut-off (low-pass) or the width (Gaussian filtering) turns out to be dependent on the strength and pulse shape of the optimal control fields. Figure 8 illustrates this dependence in the case of ideal low-pass filtering which implement the X_3 gate. The curves in Fig. 8(a) reveal that the fidelity of weaker optimal control fields is less affected by the low-pass filtering. The average absolute field amplitude specified in the legend has been calculated by averaging the absolute values of the pulse amplitudes over the total control time t_f. In contrast, the optimal fields corresponding to the fidelity curves shown in Fig. 8(b) are characterized by a similar average absolute amplitude but differ in the variance of the single absolute pulse amplitudes defined with respect to the average absolute amplitude. We see that the fidelity decays faster if the variance is larger, i.e., if the pulse amplitudes of the field are varying more rapidly. Analyzing in Fig. 8 the cut-offs at which the fidelity decays, we estimate that frequencies of up to at least twice the average absolute field amplitude are required to retain fidelities of 0.9 or larger.

To improve the results from the filtering of optimal control fields, we tried to iterate the procedure: The filtered fields are discretized and used as initial guess for the optimization algorithm. The optimal fields produced by iteration are then filtered again. In so doing we intended to generate pulses with high fidelity and even lower frequency than in the "ordinary filtering" discussed before. However, this approach does not yield significant improvements.

VI. SUMMARY AND CONCLUSIONS

Recent quantum-control studies have shown that an array of qubits coupled by nearest-neighbor Heisenberg interactions can be universally operator-controlled by acting only on the first qubit. Since these results only imply the existence of a control sequence but do not provide a way to construct them, we have investigated the feasibility of controlling a spin chain with Heisenberg interaction by applying a time-dependent magnetic field to the first spin in the chain. We have explicitly determined piecewise-constant control fields for several quantum gates for three- and four-spin chains. By increasing the number of control pulses within a fixed total time, fidelities arbitrarily close to 1 can be achieved.

We have also studied the sensitivity of the fidelity to random errors in the control fields. Our analysis shows that the average fidelity is less susceptible to random perturbations if the durations of the single control pulses are reduced. This behavior is related to a generic class of phenomena exemplified by motional narrowing in NMR. We have also examined the intrinsic saturation of the average fidelity, being universal for complete controllability and occurring if the strength of the acting random field is large enough. Finally, to make contact with experimental realizations, we have used spectral filtering to obtain smoothened control pulses retaining fidelities of 0.9.

Our study can be extended to include more complicated (e.g., continuously varying) control pulses. Such cases would require the use of some advanced methods of the optimal control theory, e.g., the Krotov algorithm, which was shown to be capable of reaching the quantum speed limit [9].

The statement that universal control of a qubit array is possible by acting on the first qubit is true in principle for arbitrarily long arrays. However, the complexity of finding the control sequence will make such a procedure impractical for Heisenberg chains. We expect our results to be of practical significance for relatively small systems of a few qubits, like those realized experimentally right now. Having fewer control lines will increase the coherence time of the qubits that are indirectly controlled by their interaction with the neighboring qubits. In the present paper, we have studied isotropic Heisenberg interactions, but the procedure also works for XXZ-type interactions. We therefore expect that our work will facilitate the control of quantum information devices with relatively few qubits.

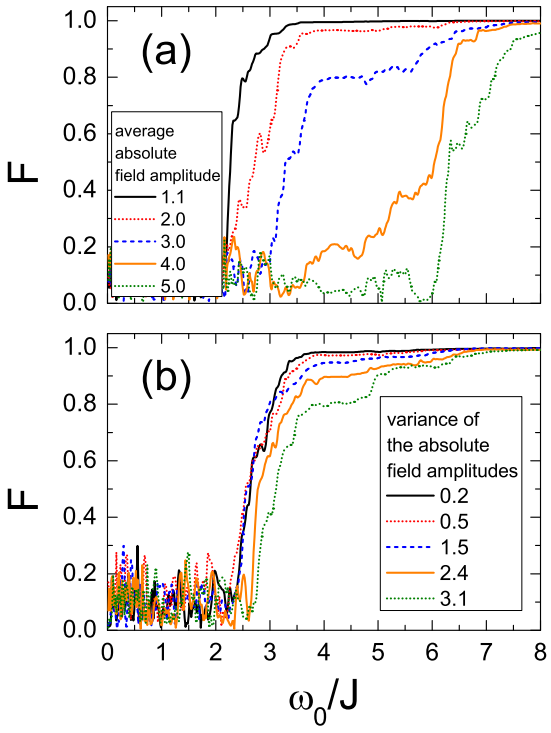

FIG. 8: (Color online) Fidelity (F) versus cut-off frequency (ω_0) for different low-pass filtered optimal control fields, all of them implementing the X_3 gate with 70 pulses of durations 1.5 alternately applied in the x and y directions: (a) The optimal control fields with average amplitudes indicated and variances ranging between 1.1 and 1.3. (b) The optimal control fields with average amplitudes between 1.9 and 2.1, and variances specified in the legend.

Acknowledgments

This work was financially supported by EU project SOLID, the EPSRC grant EP/F043678/1, the Swiss NSF, and the NCCR Nanoscience.

Appendix A: Fidelity calculation for smoothened control fields

In order to determine the fidelity corresponding to the smoothened control fields, we have to calculate the time-evolution operator $\widetilde{U}(t)$ governed by the Hamiltonian $\widetilde{H}(t) = H_0 + \widetilde{h}_x(t)S_{1x} + \widetilde{h}_y(t)S_{1y}$. One possible approach to this problem is solving the equation of motion for $\widetilde{U}(t)$, which can be written as a system of d^2 coupled first-order differential equations

$$i\frac{d}{dt}\widetilde{U}_{kl}(t) = \sum_{j=1}^{d}\widetilde{H}_{kj}(t)\widetilde{U}_{jl}(t) \quad (k,l=1,...,d)\,, \qquad \text{(A1)}$$

with $\widetilde{U}_{kl}(0) = \delta_{kl}$. While Runge-Kutta-type methods are commonly utilized for solving such systems, they are not so convenient in the case at hand where it is essential to preserve the unitarity of the time-evolution operator. We therefore determine $\widetilde{U}(t_f)$ using a product-formula approximation which manifestly preserves unitarity and essentially amounts to a discretization in time.

We divide each time interval of length T into m_T steps of length $\tau \equiv T/m_T$; the total number of steps is denoted by $m_f \equiv N_t m_T$. The approximation hinges

on the assumption that during each time step the total Hamiltonian of the system remains constant, i.e., time-independent. In other words

$$\widetilde{H}(t) = H^{(k)} \equiv H_0 + \widetilde{h}_x(k\tau)S_{1x} + \widetilde{h}_y(k\tau)S_{1y} \qquad \text{(A2)}$$

for $k\tau \leq t < (k+1)\tau$, with $k = 0, \ldots, m_f - 1$. Hence the evolution of the system during the $(k+1)$-th interval is described by $U^{(k)}(\tau) \equiv e^{-iH^{(k)}\tau}$. Using the semigroup property of time-evolution operators, $\widetilde{U}(t_f)$ can be expressed as the product

$$\widetilde{U}(t_f) = e^{-iH^{(m_f-1)}\tau} \cdot \ldots \cdot e^{-iH^{(1)}\tau} \cdot e^{-iH^{(0)}\tau}\,, \qquad \text{(A3)}$$

where each of the operators $e^{-iH^{(k)}\tau}$ is found using the spectral representation (recall Sec. II B). This approximation becomes progressively more accurate with decreasing τ, so that the time-evolution operator can be computed to the required accuracy. The unitarity of the time-evolution operator is preserved by construction for an arbitrary number of time steps, hence the method is unconditionally stable [33].

[1] M. A. Nielsen and I. L. Chuang, *Quantum Computation and Quantum Information* (Cambridge University Press, Cambridge, 2000).

[2] D. D'Alessandro, *Introduction to Quantum Control and Dynamics* (Taylor & Francis, Boca Raton, 2008).

[3] V. Jurdjevic and H. J. Sussmann, J. Differ. Equations **12**, 313 (1972); V. Ramakrishna *et al.*, Phys. Rev. A **51**, 960 (1995).

[4] H. Rabitz, M. M. Hsieh, and C. M. Rosenthal, Science **303**, 1998 (2004); H. Rabitz, T.-S. Ho, M. Hsieh, R. Kosut, and M. Demiralp, Phys. Rev. A **74**, 012721 (2006).

[5] See, e.g., S. Bose, Phys. Rev. Lett. **91**, 207901 (2003); Contemp. Phys. **48**, 13 (2007).

[6] A. Romito, R. Fazio, and C. Bruder, Phys. Rev. B **71**, 100501(R) (2005).

[7] A. O. Lyakhov and C. Bruder, Phys. Rev. B **74**, 235303 (2006); A. O. Lyakhov, D. Braun, and C. Bruder, Phys. Rev. A **76**, 022321 (2007).

[8] D. Burgarth, Eur. Phys. J. Special Topics **151**, 147 (2007).

[9] T. Caneva *et al.*, Phys. Rev. Lett. **103**, 240501 (2009).

[10] K. Maruyama, T. Iitaka, and F. Nori, Phys. Rev. A **75**, 012325 (2007).

[11] S. G. Schirmer, I. C. H. Pullen, and P. J. Pemberton-Ross, Phys. Rev. A **78**, 062339 (2008).

[12] D. Burgarth, S. Bose, C. Bruder, and V. Giovannetti, Phys. Rev. A **79**, 060305(R) (2009).

[13] A. Kay and P. J. Pemberton-Ross, Phys. Rev. A **81**, 010301(R) (2010); D. Burgarth *et al.*, *ibid.* **81**, 040303(R) (2010).

[14] X. Wang, A. Bayat, S. G. Schirmer, and S. Bose, Phys. Rev. A **81**, 032312 (2010).

[15] S. Montangero, T. Calarco, and R. Fazio, Phys. Rev. Lett. **99**, 170501 (2007).

[16] R. Fisher, F. Helmer, S. J. Glaser, F. Marquardt, and T. Schulte-Herbrüggen, Phys. Rev. B **81**, 085328 (2010).

[17] R. Heule, Master's thesis, University of Basel (2010).

[18] T. Schulte-Herbrüggen, A. Spörl, N. Khaneja, and S. J. Glaser, Phys. Rev. A **72**, 042331 (2005).

[19] M. Grace *et al.*, J. Phys. B: At. Mol. Opt. Phys. **40**, S103 (2007); M. Lapert, Y. Zhang, M. Braun, S. J. Glaser, and D. Sugny, Phys. Rev. Lett. **104**, 083001 (2010).

[20] P. T. Callaghan, *Principles of Nuclear Magnetic Resonance Microscopy* (Clarendon Press, Oxford, 1991).

[21] S. G. Schirmer, H. Fu, and A. I. Solomon, Phys. Rev. A **63**, 063410 (2001).

[22] W. H. Press, S. A. Teukolsky, W. T. Vetterling, and B. P. Flannery, *Numerical Recipes in Fortran 77 and 90: The Art of Scientific and Parallel Computing* (Cambridge University Press, Cambridge, 1997).

[23] S. G. Schirmer and P. J. Pemberton-Ross, Phys. Rev. A **80**, 030301 (2009).

[24] J. Ghosh and M. R. Geller, Phys. Rev. A **81**, 052340 (2010).

[25] M. A. Nielsen, Phys. Lett. A **303**, 249 (2002); L. H. Pedersen, N. M. Møller, and K. Mølmer, *ibid.* **367**, 47 (2007).

[26] W. Pfeifer, *The Lie Algebras su(N): An Introduction* (Birkhäuser, Basel, 2003).

[27] E. Bagan, M. Baig, and R. Muñoz-Tapia, Phys. Rev. A **67**, 014303 (2002).

[28] S. Dattagupta, *Relaxation phenomena in condensed matter physics* (Academic Press, Orlando, 1987).

[29] S. Chaudhury *et al.*, Phys. Rev. Lett. **99**, 163002 (2007).

[30] H. Jirari, F. W. J. Hekking, and O. Buisson, Europhys. Lett. **87**, 28004 (2009).

[31] J. Werschnik and E. K. U. Gross, J. Phys. B: At. Mol. Opt. Phys. **40**, R175 (2007).

[32] I. S. Gradshteyn and I. M. Ryzhik, *Tables of integrals, series and products* (Academic Press, New York, 1965).

[33] See, e.g., A. H. Hams and H. De Raedt, Phys. Rev. E **62**, 4365 (2000); H. De Raedt, A. Hams, K. Michielsen, and K. De Raedt, Comp. Phys. Commun. **132**, 1 (2000).